Optical Signatures of Energy-Level Statistics in a Disordered Quantum System

V. Savona, S. Haacke, and B. Deveaud

Physics Department, Swiss Federal Insitute of Technology Lausanne, CH-1015 Lausanne-EPFL, Switzerland

(Received 26 May 1999)

Time-resolved measurements of the resonant Rayleigh scattering from quantum well excitons are shown to provide information on the energy-level statistics of the localized exciton states. The signal transients are reproduced by a microscopic quantum model of the exciton two-dimensional motion in presence of spatially correlated disorder. This model allows quantitative determination of the average energy separation between the localized states. Here this quantity turns out to be only a few times smaller than the average disorder amplitude, proving that spatial correlation and quantum mechanics are equally important in the description of the exciton localization process.

PACS numbers: 78.47.+p, 71.23.–k, 71.35.–y, 78.66.–w

The study of the fundamental properties of disordered systems mostly relies on transport measurements in metals [1]. In these systems, however, the density of carriers is fixed and the physics is governed by the strong interplay between disorder and many-body Coulomb correlations [2]. In addition, transport measurements probe the highest occupied energy levels, close to the Fermi energy, which are only weakly affected by the underlying disorder. On the theoretical side, a general understanding of many-body disordered systems is far from being achieved [2] (see, e.g., the recent debate on interaction-induced delocalization of electrons [3]). Besides, many aspects of single-particle disordered quantum systems, such as weak localization in two dimensions or the effects of spatial correlation, still leave open questions. For this reason, an experimental environment with noninteracting particles would be of great interest for the understanding of the basic aspects in the physics of disorder and localization. Excitons in semiconductor heterostructures could be eligible for such a role. Indeed, excitons are globally neutral and their mutual dipole-dipole interaction has thus a shorter range. Furthermore, excitons are produced by optical excitation and their density can be adjusted within a wide range. This allows one to minimize many-body effects and basically perform experiments in an ideal noninteracting regime. Finally, excitons are probed by means of optical spectroscopy. The selection rules for the optical transitions imply that only the lowest exciton levels—those mostly subject to localization—are probed.

Resonant Rayleigh scattering (RRS) [4] of light on quantum well excitons has been the subject of many experimental [5–9] and theoretical [10–12] investigations in the past years. Disorder in a quantum well (QW), provided by interface roughness, results in an effective two-dimensional potential with spatial correlation which localizes the center of mass of the exciton [10,13]. It is now well established that, in the limit of low excitation density and linear optical response, RRS due to disorder is the dominant contribution to the emission into nonspecular directions (secondary emission) [14,15]. However, the connection between the scattering cross section and the two-point spectral correlation function of the disordered system has been overlooked so far. Recently, it has been suggested [16] that the RRS transient following an ultrashort light pulse allows a direct measurement of the statistical distribution of the energy-level distances of the two-dimensional exciton center-of-mass (COM) motion. This establishes a direct relationship between RRS transient and quantum mechanical exciton localization, allowing one to obtain quantitative information about the average quantization energy (denoted energy-level repulsion) characteristic of excitons lying in the same localization site.

In this Letter we present time-resolved measurements of RRS displaying new features that we attribute to the energy-level repulsion. This quantity had previously been investigated by means of spectroscopic techniques with microscopic spatial resolution [17]. We prove that the level repulsion can be inferred from the macroscopic optical response. In order to support this interpretation, we extend the microscopic theory of QW exciton RRS, based on the solution of the COM Schrödinger equation, to the two-dimensional case [16]. All the measured transients are well reproduced by the numerical calculations. By comparing theory and experiment, we gather information on the exciton level statistics and provide an estimate of the spatial correlation length of the disordered potential.

The excitonic transitions in four different samples have been resonantly excited by means of an ultrashort light pulse. The intensity of the secondary emission is measured in a two-color luminescence up-conversion experiment with a temporal resolution of 150 fs and an improved sensitivity [7]. Excitation and detection were linearly copolarized. The sample temperature was 18–20 K. The four samples under investigation, denoted A, B, C, and D, are molecular-beam-epitaxy-grown multiple QW $GaAs/Al_{0.7}Ga_{0.7}As$ structures coming from different growth facilities, having well widths of 12 (A), 13 (B), 10.5 (C), and 10 (D) nm, and displaying photoluminescence linewidths of 1.2 (A), 1.0 (B), 1.8 (C), and 2.2 (D) meV. Figure 1(a) shows the measured time-dependent RRS intensities. These transients are obtained for estimated excitation densities $<10^9$ cm^{-2},

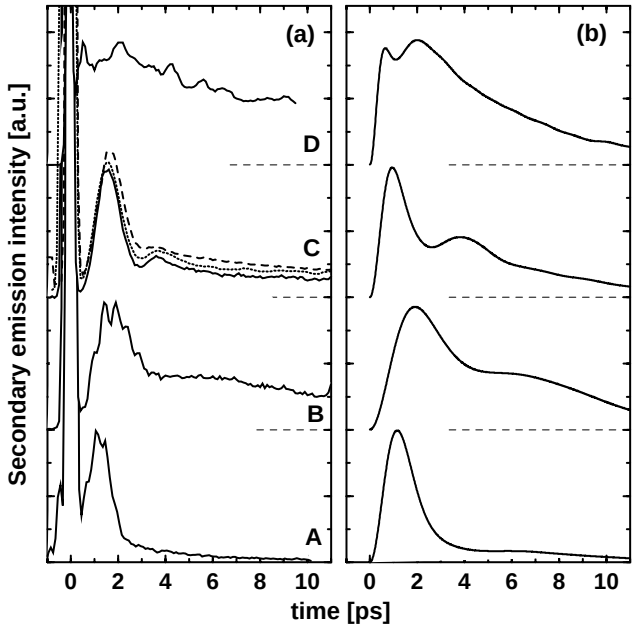

FIG. 1. (a) measured and (b) calculated RRS signals. Experimental data for sample C are plotted for excitation density 10^8 cm^{-2} (full line), 2.5×10^8 cm^{-2} (dotted line), and 5×10^9 cm^{-2} (dashed line), normalizing the intensity of the main peak and introducing a small shift of the vertical axis.

such that density effects may be neglected. As a check, we plot the signal of sample C taken at three different excitation densities. The shape of the signal is unchanged in the range of densities studied, thus confirming that the measurement is done in the linear response regime. Similar checks have been done for the other samples. After the initial sharp peak that originates from surface nonresonant Rayleigh scattering, the four signals rise up to a first maximum occurring at times varying like the inverse of the respective exciton inhomogeneous broadening. Afterwards, sample A displays a fast and then a slow decay component. Sample B is characterized by a plateau between the fast and slow decaying parts, while the modulations appearing at early times originate from heavy-light hole exciton beats [11]. In the case of sample C, the plateau is replaced by a second distinct maximum. The signal of sample D has an irregular shape because of residual time speckles [15] due to a small angular detection window used for that particular sample. However, a clear envelope can still be identified.

RRS theories based on the classical exciton in-plane motion predict a single maximum in the time-dependent signal, followed by a monotonic decay [10]. A quantum mechanical treatment based on a perturbative approach [11] has predicted a RRS transient significantly different from the classical limit, although a monotonic decay is always present. Here, we show that the observed features can be explained within a semiclassical theory of RRS based on a full numerical solution of the quantum mechanical in-plane exciton motion. In a QW, disorder results in fluctuations of the electron and hole confinement energies. It has been shown [10,13] that, provided the amplitude of these fluctuations is smaller than the exciton binding energy, disorder affects significantly only the exciton COM motion, through an effective potential $V(\mathbf{r})$. Under this assumption, the linear exciton susceptibility reads [18]

$$\chi(\mathbf{r}, \mathbf{r}', z, z', \omega) = \frac{\mu_{cv}^2 |F_{1S}(0)|^2}{\hbar} \rho(z)\rho(z')G(\mathbf{r}, \mathbf{r}', \omega), \tag{1}$$

where $\rho(z)$ is the product of the electron and hole envelope functions along the growth axis and the factors preceding $\rho(z)$ account for the exciton optical matrix element [19]. The quantity $G(\mathbf{r}, \mathbf{r}', \omega)$ is the retarded propagator for the exciton COM motion. Maxwell equations can be solved assuming an incoming plane wave with in-plane wave vector $\mathbf{k}_{\text{in}}$ and an outgoing plane wave $\mathbf{k}_{\text{out}}$, in the far field approximation. By neglecting retardation (polaritonic) corrections along the in-plane direction [12], the scattering amplitude is simply the propagator G in reciprocal space. By Fourier transforming $G(\mathbf{r}, \mathbf{r}', \omega)$ with respect to its first argument, the propagator $G(\mathbf{k}_{\text{in}}, \mathbf{r}, \omega)$ obeys the following Dyson's equation:

$$(H_{\mathbf{r}} - \hbar\omega - i\gamma)G(\mathbf{k}_{\text{in}}, \mathbf{r}, \omega) = e^{i\mathbf{k}_{\text{in}}\cdot\mathbf{r}}, \tag{2}$$

where $H_{\mathbf{r}} = -(\hbar^2/2M)\Delta_{\mathbf{r}} + V(\mathbf{r}) + \hbar\omega_0$ is the exciton COM motion Hamiltonian and $\hbar\omega_0$ the central exciton energy. The potential $V(\mathbf{r})$ is randomly generated in order to be Gauss distributed and Gauss correlated in space according to

$$\langle V(\mathbf{r})V(\mathbf{r}')\rangle = \sigma^2 e^{-(\mathbf{r}-\mathbf{r}')^2/2\xi^2}. \tag{3}$$

Here, $\langle\cdots\rangle$ denotes ensemble average over random configurations, σ is the width of the energy distribution, and ξ is the correlation length characterizing the potential fluctuations. For QW excitons, this effective potential is a result of the convolution of the actual electron and hole confinement potential with the $1S$ exciton wave function $F_{1S}(\mathbf{R})$ [10]. Thus, the exciton Bohr radius a_B is a lower bound to the correlation length ξ. The choice of a Gauss correlation function is only made in order to simplify the numerical solution of the Schrödinger equation. In reality, the correlation function is not expected to be strictly of Gaussian shape [9,10]. However, the Gauss form shows to be a satisfactory choice to give the general physical ground for the interpretation of the present measurements. Equation (2) has been solved on a grid of $2^8 \times 2^8$ points spanning a square region of 1 μm^2. Fourier transforming with respect to $\mathbf{r}$ and ω gives the time-dependent scattering amplitude $G(\mathbf{k}_{\text{in}}, \mathbf{k}_{\text{out}}, t)$. Equation (2) is numerically solved for each independent realization of $V(\mathbf{r})$, the scattered field is calculated, and its time-dependent intensity is finally averaged over statistically independent potential realizations. We point out that a configuration average in this case is not related to any ergodic assumption, contrary to what has recently been argued [8]. Rather, as can be easily checked [16], it is justified by the large angular acceptance of the experimental setup. Figure 1(b) shows

the RRS intensity $I(t) \propto |G(\mathbf{k}_{\text{in}}, \mathbf{k}_{\text{out}}, t)|^2$ calculated for $\mathbf{k}_{\text{in}} = 0$ and $\mathbf{k}_{\text{out}} = 6.6 \times 10^{-3}$ nm^{-1}, corresponding to a 45° external emission angle. The configuration-averaged result does not depend on $\mathbf{k}_{\text{out}}$ within the external emission cone, as expected for $\xi \ll \lambda$. A very good agreement between theory and experiment emerges from the comparison of Figs. 1(a) and 1(b). We attribute the small quantitative discrepancies to the rather simplistic assumption of a Gauss correlated disorder. For all the calculated transients, the mass was $M = 0.25m_0$, and $\gamma = 80$ μeV. This latter was adjusted to reproduce the exponential decay occurring after the RRS transient. The parameter σ was chosen in order to reproduce for each sample the measured spectral width [20]. The values used are $\sigma = 0.65$ (A), 0.39 (B), 0.85 (C), and 1.2 (D) meV. The correlation length ξ has been adjusted to fit the results to the measured transients. The values used to reproduce the experimental data are $\xi = 70$ (A), 45 (B), 40 (C), and 23 (D) nm, corresponding to $\sigma/E_c = 26.6$ (A), 5.7 (B), 10.0 (C), and 4.2 (D). These values for ξ are considerably larger than the exciton Bohr radius, suggesting an interface structure with a flat island extending over about 100 nm. This picture agrees well with independent measurements of the typical island geometry for good quality samples, based on microphotoluminescence and atomic force microscopy [17]. To our knowledge, this is the first time such information can be drawn from a macroscopic measurement.

Alternative mechanisms [21,22] being known to give rise to peculiar features in the time-dependent secondary emission can be ruled out in the present case. In particular, the linearity of the measured signals, within the range of excitation densities here considered ($<10^9$ cm^{-2}), allows us to rule out Coulomb correlation effects. Recently, [21] it has been predicted that such effects are always accompanied by a significant variation of the transient shape and by a nonlinear dependence of the signal intensity, as a function of the excitation density. Acoustic phonon relaxation mechanisms are excluded on the basis of their long characteristic time at low temperature, as compared to the short time scale of RRS. Polaritonic or propagation effects might originate from the interplay between retardation and multiple interference in the signal propagation along the z axis [22], giving rise to modulations in the time dependent reflection and transmission. A straightforward extension of the present model to account for multiple QW structures and propagation effects (the details of this formalism will be the subject of a future publication) has allowed us to test the relevance of this effect. For the parameters of the four structures here considered, no significant propagation effects appear in the simulated RRS transients.

In order to understand the physics behind these results, we derive the connection between RRS and the statistical distribution of energy levels of the COM motion. It has been shown [16] that the configuration-averaged time-dependent RRS intensity is the Fourier transform of the statistical distribution of the exciton energy-level separations weighted with the optical matrix element:

$$R_c(E) = \frac{1}{\Omega}\left\langle \sum_{n,m} M_n^2 M_m^2 \delta(E - \hbar(\omega_n - \omega_m)) \right\rangle - \Omega \int dE'\, D(E') D(E' - E), \tag{4}$$

where $D(E) = (1/\Omega)\langle \sum_n M_n^2 \delta(E - \hbar\omega_n)\rangle$ is the exciton optical density, corresponding to the absorption spectrum, $M_n = \int \phi_n(\mathbf{r})\, d\mathbf{r}$ is the exciton-electromagnetic field overlap integral of the nth exciton level at normal incidence, and Ω is the surface of the system. Here, $\phi_n(\mathbf{r})$ and $\hbar\omega_n$ are, respectively, the nth eigenfunction and eigenvalue of $H_{\mathbf{r}}$. Expression (4) represents a two-point average minus its uncorrelated counterpart. Thus, $R_c(E)$ is a measure of the correlation in the energy-level statistics. It would vanish in the case of a completely random energy-level distribution, while positive (negative) values indicate that the energy-level separation E is statistically more (less) frequent than average. Because of the scaling properties of the Schrödinger equation, the relevant parameter which determines the shape of the quantities $I(t)$ and $R_c(E)$ upon rescaling is σ/E_c, where $E_c = \hbar^2/2M\xi^2$ is a measure of the level spacing in a potential well of width ξ [16]. The limit $\sigma/E_c \gg 1$ corresponds to classical exciton COM motion. The opposite situation $\sigma/E_c \ll 1$ represents the *white noise* limit, where wave functions extend over several potential fluctuations and spatial correlation is no longer relevant. This distinction is schematically depicted in Fig. 2(d).

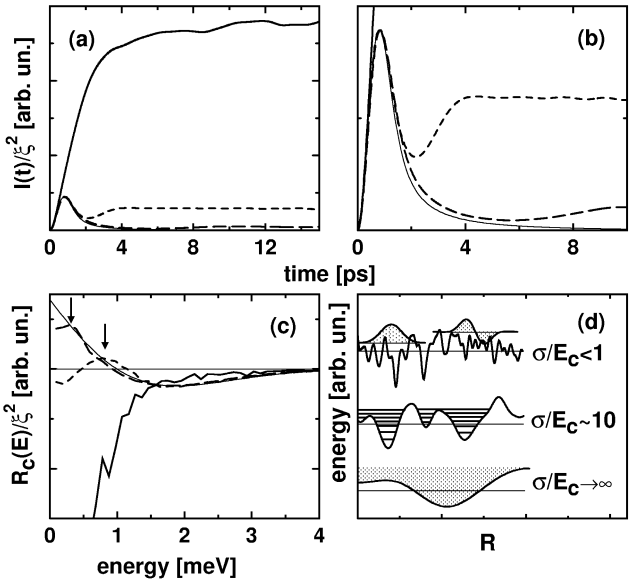

FIG. 2. (a) Time-dependent RRS calculated for $\sigma/E_c = 1$ (solid line), $\sigma/E_c = 10$ (short dashed line), $\sigma/E_c = 100$ (long dashed line), and the classical limit $\sigma/E_c \to \infty$ (thin solid line). (b) Blowup of (a). (c) Level statistics $R_c(E)$ corresponding to the curves in (a) and (b). (d) Schematic representation of the physical situations corresponding to different limiting values of σ/E_c.

In Figs. 2(a) and 2(b) we plot the scaled $I(t)$ corresponding to $\sigma/E_c = 1$, 10, 100, together with the classical limit $\sigma/E_c \to \infty$ which obeys an analytical expression [11]. Correspondingly, Fig. 2(c) shows the optical energy-level correlation $R_c(E)$. Both quantities have been calculated using the (unphysical) value $\gamma = 0$. This results in a finite limiting value of $I(t)$ at long times, except the classical curve that decays according to t^{-2} [11]. For large values of σ/E_c, the first maximum coincides with the classical result. However, at later times the signal presents a minimum. The position of this minimum as well as the intensity ratio between the limiting value and the classical peak directly depend on σ/E_c [16]. It is clear that such a behavior can easily explain our RRS data, once an overall damping factor $e^{-2\gamma t}$ is included. We remark that our fit gave $\sigma/E_c > 1$ for all samples. The exciton in-plane motion thus displays intermediate features between the classical and the white noise limits.

The RRS transients have their counterpart in $R_c(E)$, plotted in Fig. 2(c). While the classical curve has a positive maximum at $E = 0$ originating from the spatial correlation, all the other curves show a dip, due to quantum mechanical level repulsion. In particular, for small values of σ/E_c wave functions are localized on a scale larger than ξ [top sketch in Fig. 2(d)] and all the eigenstates are mutually subject to the level repulsion, resulting in a negative value of $R_c(E)$ for all energies. For increasing values of σ/E_c the numerical results for $R_c(E)$ approach the classical limit. This limit is first approached by large values of E, while a dip always remains for $|E| \to 0$, reflecting level repulsion between spatially overlapping states. In these intermediate situations, a maximum at $E \simeq E_c$ appears [arrows in Fig. 2(c)]. This maximum originates from the preferential value E_c taken by the level spacing, due to the typical lateral size ξ of the minima in the disordered potential [middle sketch in Fig. 2(d)]. The maximum in $R_c(E)$ corresponds to an oscillation in time domain around the finite limiting value taken by $I(t)$ at long times. Indeed, the minimum and revival in the dashed curves of Figs. 2(a) and 2(b) are just the first half period of this oscillation which is rapidly damped because of the broadening of the peak in $R_c(E)$. In practice, the oscillation is due to interference between the fields emitted by the different oscillators with a statistically dominant level spacing E_c. This interpretation finally shows the intimate connection between the shape of the RRS transient and the level statistics of the underlying disordered one-particle system.

In conclusion, we have presented time-resolved measurements of the secondary emission from QW excitons under resonant fs excitation. A microscopic RRS model with spatially correlated disorder provides a clear interpretation in terms of the quantum mechanical energy-level spacing between localized exciton states. The quantum mechanical description of the exciton COM propagation is thus essential to correctly describe the polarization dynamics. Our analysis confirms previous expectations of the size of the correlation length characterizing interface fluctuations in the epitaxial growth process. The secondary emission from QWs under low excitation conditions turns out to be a direct probe of the microscopic features of a one-particle disordered quantum system in two dimensions, thus opening a new range of possibilities for the study of the physics of disorder.

This work was partially supported by the Swiss Priority Project "Optics."

[1] B. Kramer and A. MacKinnon, Rep. Prog. Phys. **56**, 1469 (1993).
[2] P. A. Lee and T. V. Ramakrishnan, Rev. Mod. Phys. **57**, 287 (1985); D. Belitz and T. R. Kirkpatrick, Rev. Mod. Phys. **66**, 261 (1994).
[3] F. von Oppen *et al.,* Phys. Rev. Lett. **76**, 491 (1996); R. A. Römer *et al.,* Phys. Rev. Lett. **78**, 515 (1997); T. Vojta *et al.,* Phys. Rev. Lett. **81**, 4212 (1998).
[4] R. Loudon, *The Quantum Theory of Light* (Oxford Science Publications, Oxford, 1983).
[5] H. Stolz, *Time-Resolved Light Scattering from Excitons,* Springer Tracts in Modern Physics Vol. 130 (Springer, Berlin, 1994).
[6] J. Hegarty *et al.,* Phys. Rev. B **30**, 7346 (1984); J. Hegarty and M. D. Sturge, J. Opt. Soc. Am. B **2**, 815 (1985); H. Stolz and D. Schwarze *et al.,* Phys. Rev. B **47**, 9669 (1993); M. Gurioli *et al.,* Solid State Commun. **97**, 389 (1995); N. Garro *et al.,* Phys. Rev. B **55**, 13 752 (1997); H. Wang, *et al.,* Phys. Rev. Lett. **74**, 3065 (1995); M. Woerner, *et al.,* Phys. Rev. Lett. **81**, 4208 (1998).
[7] S. Haacke *et al.,* Phys. Rev. Lett. **78**, 2228 (1997).
[8] D. Birkedal and J. Shah, Phys. Rev. Lett. **81**, 2372 (1998).
[9] A. V. Shchegrov *et al.,* Phys. Rev. Lett. **83**, 1391 (1999).
[10] R. Zimmermann, Phys. Status Solidi (b) **173**, 129 (1992).
[11] R. Zimmermann, Nuovo Cimento Soc. Ital. Fis. **17D**, 1801 (1995).
[12] D. S. Citrin, Phys. Rev. B **54**, 14 572 (1996).
[13] S. D. Baranovskii *et al.,* Phys. Rev. B **48**, 17 149 (1993).
[14] M. Gurioli *et al.,* Phys. Rev. Lett. **78**, 3205 (1997).
[15] W. Langbein *et al.,* Phys. Rev. Lett. **82**, 1040 (1999).
[16] V. Savona and R. Zimmermann, Phys. Rev. B **60**, 4928 (1999).
[17] K. Brunner *et al.,* Phys. Rev. Lett. **73**, 1138 (1994); D. Gammon *et al.,* Phys. Rev. Lett. **76**, 3005 (1996); U. Jahn *et al.,* Phys. Rev. B **54**, 2733 (1996).
[18] R. Kubo, J. Phys. Soc. Jpn. **12**, 570 (1957).
[19] F. Tassone *et al.,* Nuovo Cimento Soc. Ital. Fis. **12D**, 1673 (1990).
[20] The exciton spectral width is 2.35σ in the classical limit and shows a weak narrowing for decreasing ξ [11]. Theory accounts only for lateral disorder and reproduces the measured linewidths within 20% accuracy. The difference can be attributed to vertical disorder in these multiple QWs.
[21] M. Kira *et al.,* Phys. Rev. Lett. **82**, 3544 (1999).
[22] J. J. Baumberg *et al.,* Phys. Rev. Lett. **80**, 3567 (1998); L. C. Andreani *et al.,* Phys. Rev. B **57**, 4670 (1998).